UNIVERSAL CORRELATIONS OF NUCLEAR OBSERVABLES AND NEW SIGNATURES OF STRUCTURE IN EXOTIC NUCLEI: A REVIEW

R.F. CASTEN

Brookhaven National Laboratory, Upton, New York 11973, USA
Yale University, New Haven, Connecticut 06511, USA

N.V. ZAMFIR

Brookhaven National Laboratory, Upton, New York 11973, USA
Clark University, Worcester, Massachusetts 01610, USA
Institute of Atomic Physics, Bucharest-Magurele, Romania

ABSTRACT

Recently, several nearly universal correlations of nuclear observables, spanning nuclei from singly magic to rotor, have been discovered. The simple global behavior revealed by these correlations discloses new signatures of structure that require a knowledge only of the energies of the first two excited states in even-even nuclei and the $B(E2 : 2_1^+ \rightarrow 0_1^+)$ value. Since these are the simplest- to-obtain data in new nuclei in unexplored regions, they should be especially valuable in radioactive beam studies of nuclei far from stability where the data will necessarily be sparse compared to that with which we are accustomed. This report reviews some of these recent developments.

1. Introduction

Traditionally, nuclear structure is viewed in a "vertical" sense in terms of the excitations in a specific nucleus or in a small region of nuclei. Virtually all models and experiments are designed to look at nuclear structure in this way. Yet, the present situation in nuclear physics offers an alternative approach. Over the years, a tremendous body of nuclear structure data has been built up through countless experiments and a number of different types of structure have been identified such as nuclei near closed shells, vibrational nuclei, rotational nuclei, and many varieties of intermediate forms. The vast reservoir of data now offers a unique opportunity to explore nuclear structure in a *horizontal or evolutionary* way.

This can be done by studying *correlations* of collective observables either with external quantities or with other collective observables. From studies of these correlations a growing realization has emerged in the last decade that the seemingly-complex evolution of structure across the nuclear chart can in fact be viewed very simply. The compact and simple correlations that are disclosed pose one of the greatest challenges today to modern theories of nuclear structure.

A horizontal perspective can provide new signatures of structure that are based on the easiest-to-obtain data. This development has the potential for significant

impact in the era of radioactive nuclear beams (RNBs) since experiments with RNBs will never yield the quantity and variety of data in particular nuclei that we are accustomed to. The recent extension of various correlation schemes from regional (neutron, proton half shells) to global (e.g., $Z = 30 - 100$) character is especially important in this regard.

2. The N_pN_n scheme and the P-factor

As noted, nuclear data is often bewildering in its complexity. This is illustrated on the left in Fig. 1 which shows 2_1^+ energies in the $A = 100$ region. The phenomenology shows a large range of $E(2_1^+)$ values and a variety of structures but certainly does not disclose any simple way to "see" this structural evolution. Of course, detailed models can be applied to regions like this so that the details of Fig. 1 can be understood: for example, a spherical-deformed transition occurs most rapidly in Sr, Zr, less so in Mo and hardly at all in Cd. Yet such detailed calculations, though valuable, belie the point of seeking a simple ansatz for the systematics and are seldom done in the absence of sufficient pre-existing data for a given region that its structural features are already clear.
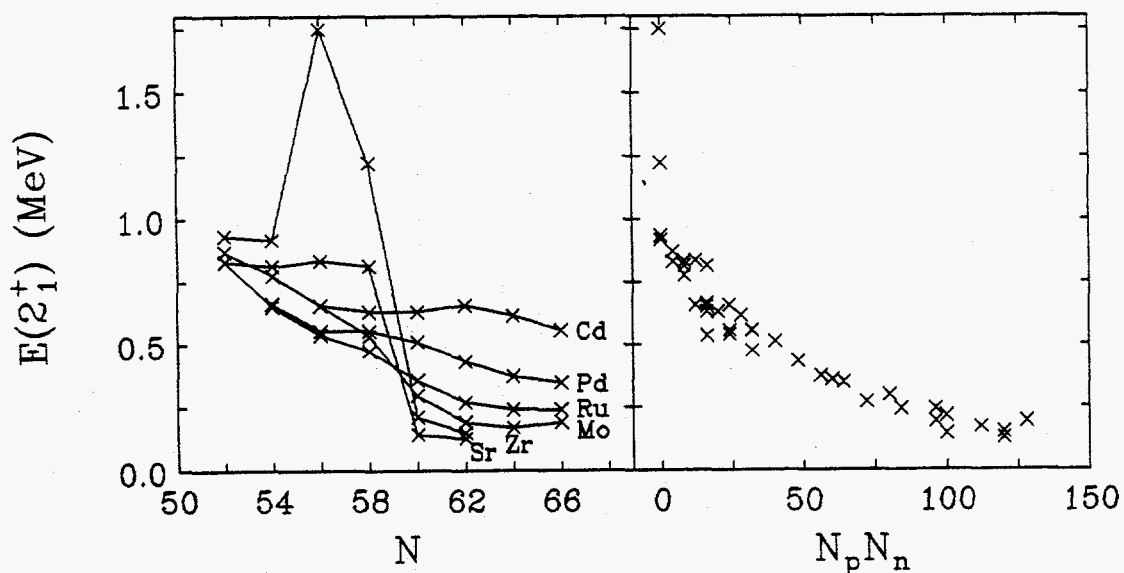

Fig. 1. Normal and N_pN_n plots for $E(2_1^+)$ values near $A = 100$.

DISCLAIMER

DISCLAIMER

Portions of this document may be illegible electronic image products. Images are produced from the best available original document.

We take a different approach. It is well known that the valence $p-n$ interaction is critical to the development of collectivity.[1] Hence, one might expect that there should be some relatively simple quantity that embodies the principal effects of the $p-n$ interaction and that the evolution of nuclear structure might be simple if parameterized according to such a variable. If we assume that the integrated valence $p-n$ interaction is not sensitive to details of orbit occupation (a rough approximation which is approximately confirmed empirically) then it should scale as the product of the number of valence protons, N_p, and the number of valence neutrons, N_n; that is, by the valence product $N_p N_n$. Note that N_p and N_n are counted, either as particles or holes, to the nearest closed shells. Correlations of mean field observables with $N_p N_n$ are the essence of what is known as the $N_p N_n$ scheme[2], illustrated on the right side of Fig. 1. Evidently, there is a profound simplification. Similar plots are obtained for other observables such as $R_{4/2} \equiv E(4_1^+)/E(2_1^+)$, $B(E2 : 2_1^+ \rightarrow 0_1^+)$. The only caveat is that in constructing such plots attention must be paid to the presence, and evolution, of important subshell closures which affect the counting of valence nucleons. The $A = 100$ region provides a well known example of this. For nuclei with $N < 60$ there is a significant proton gap at $Z = 40$. However, this gap disappears suddenly (another effect of the $p-n$ interaction) for $N \geq 60$, leaving behind the traditional $Z = 28 - 50$ shell. [A similar gap occurs for $Z = 64$ in the $A = 150$ region, which disappears for $N \geq 90$.]

Many $N_p N_n$ correlations, covering most regions of nuclei, have been shown in the literature and need not be repeated here. Rather, we will turn to some newer results. Before doing so, however, it is interesting to consider one modification to $N_p N_n$. In the $N_p N_n$ scheme, due to different shell sizes, there is no obvious interpretation of a particular numerical value of $N_p N_n$. For example, does a value $N_p N_n = 120$ imply a collective deformed nucleus or not? It would be useful to have a quantity whose absolute value conveys some more precise physical idea. This goal is the motivation behind the $P - factor$ which is defined as[3]

$$P = \frac{N_p N_n}{N_p + N_n} \tag{1}$$

P is a "normalized" $N_p N_n$ giving the number of $p-n$ interactions per valence nucleon. More significantly, it is the number of valence $p-n$ interactions divided by the number of pairing interactions and is therefore proportional to the ratio of integrated strengths of these interactions. Since typical $p-n$ matrix elements are ~ 0.2 MeV, and the pairing interaction strength is ~ 1 MeV, $P \sim 5$ corresponds to the point at which the $p-n$ interaction strength begins to dominate the pairing strength. It is hardly surprising that nuclei become deformed for P values near 5.

There is an elegant way of demonstrating that P senses the competition between $p-n$ and pairing interactions. An empirical measure of this competition, the ratio ϵ/Δ, where ϵ is the usual quadrupole deformation and Δ is the average pairing gap $[\Delta = (\Delta_p + \Delta_n)/2]$, can be empirically extracted from $B(E2 : 2_1^+ \rightarrow 0_1^+)$ values and odd-even mass differences. A nearly global comparison of ϵ/Δ values with P is shown in Fig. 2. The match is excellent, even in fine details.

The significance of this is worth stressing: it is possible to account for the evolution of collectivity and the competition between deformation and spherical-driving forces without resorting to complex microscopic calculations or to multi-parameter phenomenological schemes. Instead, a very good reproduction of the behavior of virtually all nuclei from $Z = 40 - 100$ is obtained merely by multiplying two numbers and dividing by their sum.
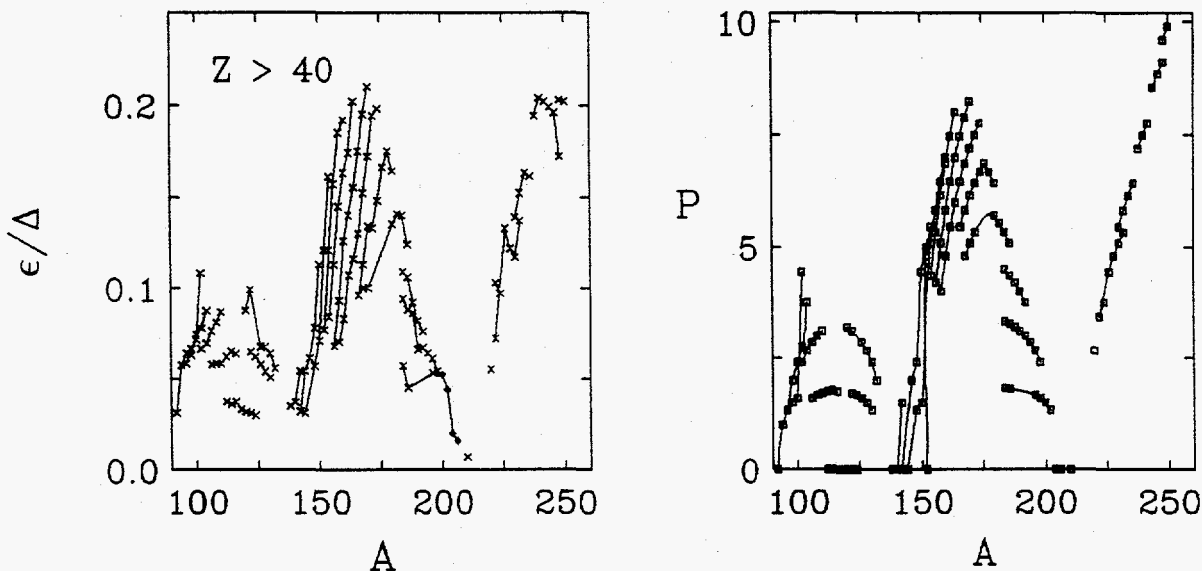

Fig. 2. Comparison of empirical ϵ/Δ and P values. Ref. 4.

3. Correlations of Collective Observables

3.1. The Anharmonic Vibrator and a Tripartite Classification of Nuclear Structure

Striking as these correlations are, correlations *between* collective observables themselves are even more remarkable. For example, consider yrast energies. Nuclei with a few particles of both kinds outside closed shells are often vibrational in character. They have high 2_1^+ energies and $E(4_1^+) \sim 2E(2_1^+)$. At another extreme of structure, at very low $E(2_1^+)$ values, rotational nuclei have $E(4_1^+) \sim 3.33E(2_1^+)$. One would therefore expect the relation between $E(4_1^+)$ and $E(2_1^+)$ to evolve from one to the other of these extremes. Although this evolution might be rather simple for a given element, it is hardly to be expected that the $E(4_1^+) - -E(2_1^+)$ correlation will be regionally or globally simple. However, despite the general perception of

the complexity of nuclear structural evolution, a remarkably compact correlation is observed.[17] We show this in Fig. 3 which assembles all data on *collective, non-rotational* nuclei between $Z = 38$ and 82. The data fall along a straight line given by

$$E(4_1^+) = 2.0E(2_1^+) + \epsilon_4 \tag{2}$$

where $\epsilon_4 = 0.16(0.01) MeV$. This particular slope is structurally revealing. Equation 2 is that for an AnHarmonic Vibrator (AHV), where ϵ_4 is the anharmonicity ϵ_4 (deviation of $E(4_1^+)$ from the harmonic value of twice $E(2_1^+)$). That such a broad assemblage of nuclei can be well fit with a single, almost constant, anharmonicity is totally unexpected. These nuclei are definitely *not* similar in structure. They include near harmonic vibrators, γ-soft nuclei, near rotors, and all varieties of transitional nuclei. While an AHV model can indeed describe each of these types of structure *individually*, there is no reason *a priori* to expect the anharmonicity ϵ_4 to be *constant*. The meaning of constant ϵ_4 needs to be explored, but it seems to imply that despite *widely varying internal phonon structure* of the 2_1^+ level (the 1-phonon excitation), the phonon-phonon interaction remains unchanged. How this utterly simple phenomenology arises is a major challenge to microscopic theory. A clue to this understanding may be provided by the IBA which automatically reproduces the observed behavior, even with rather general Hamiltonians. [6] These IBA calculations inherently embody a good phonon structure for the yrast levels[7].
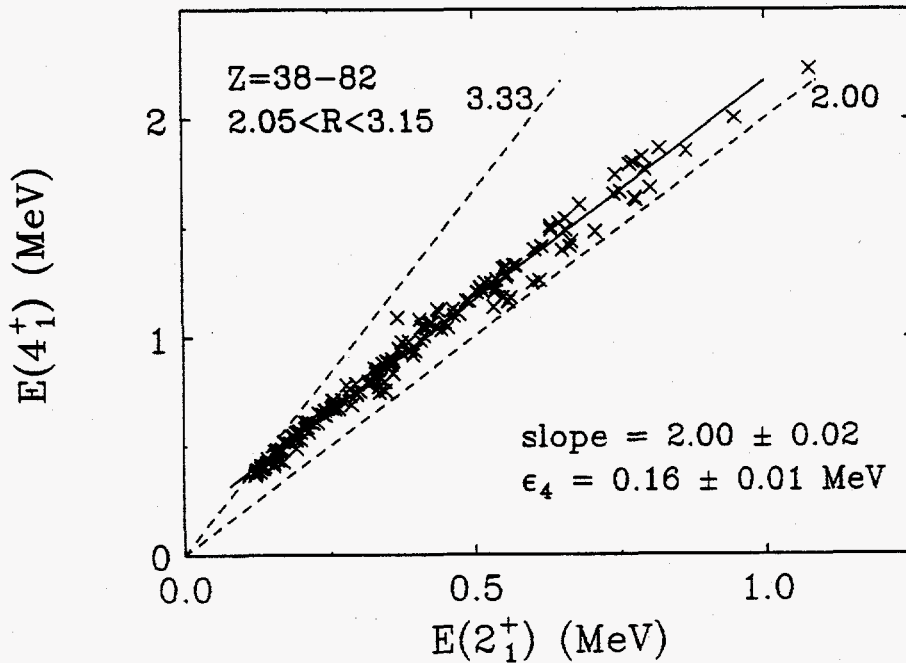

Fig. 3. Correlation of $E(4_1^+)$ with $E(2_1^+)$ for $38 \leq Z < 82$ and $2.05 \leq R_{4/2} \leq 3.15$.

It is possible to extend this kind of analysis to include all kinds of structures, including rotors and even "pre- collective" nuclei ($R_{4/2} < 2.0$). To see this, consider the trajectory in Fig. 3. Of course, the trend line with slope of 2.0 cannot continue indefinitely as $E(2_1^+)$ decreases, for otherwise the finite positive value of ϵ_4 implies that the data would cross the 3.33 rotor limit. Therefore, at some critical 2_1^+ energy the data begin to "roll over" and to merge with the rotor line. Indeed, as seen in Fig. 4, for $R_{4/2} \geq 3.15$, the data again follow a straight line with slope very close to the rotor value of 3.33. The fact that the AHV description persists down to such low $E(2_1^+)$ energies (~ 0.14 MeV), *forces* a squeezing of the *range* of 2_1^+ energies in which the transition to a rotor occurs. This enforced rapidity in turn implies that the structural transition can be described by the equations of critical phase transitional behavior of the type observed in magnetic and thermodynamic systems. That finite nuclei, whose structure is dominated by just a few valence nucleons, can exhibit such phase transitional behavior is yet another challenge to the theory of finite-body quantal systems in a nuclear context.

At the other extreme of structural evolution, that is, nuclei near closed shells, with high 2_1^+ energies, the correlation also changes but again preserves a simple pattern (see Fig. 4). For $R_{4/2} < 2.0$, the data lie on a new straight line with a slope of unity. The slope of unity can be interpreted quite simply.[8] If successive nuclei, with $n-2$ and n valence nucleons of one type, differ only in the addition of an identical zero-coupled pair of nucleons, then the change in energy of $J \neq 0$ yrast states will be the same: that is, both $E(4_1^+)$ and $E(2_1^+)$ will change identically. Thus, their energy difference remains constant which implies the equation, $E(4_1^+) = E(2_1^+) + $ constant, and hence the slope of $E(4_1^+)$ against $E(2_1^+)$ is unity as observed.
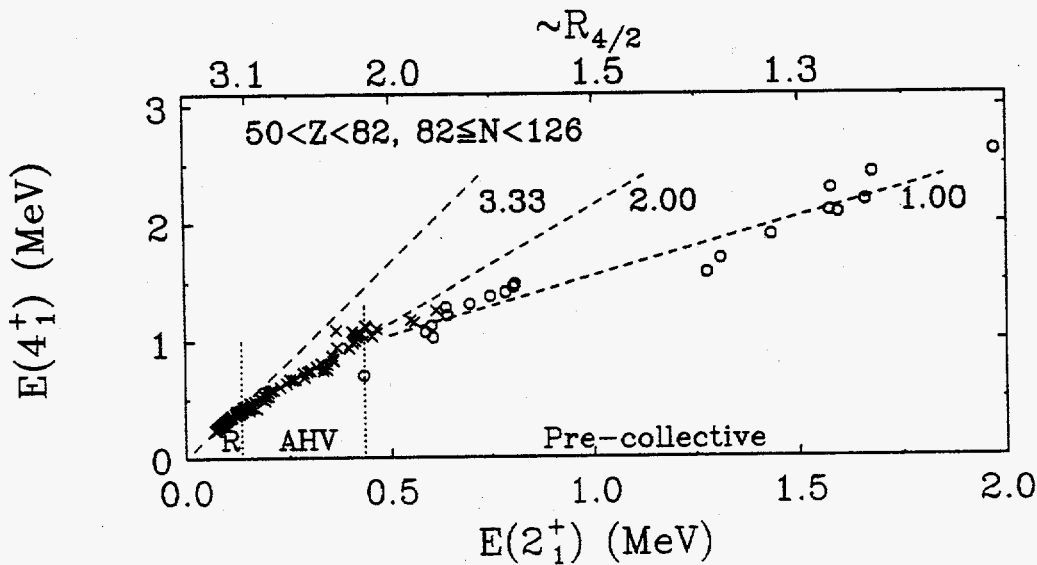

Fig. 4. Same as Fig. 3 for $Z = 50 - 82$ and all $R_{4/2}$ values.

To summarize, the evolution of structure follows a tripartite classification into rotor, AHV, and "pair addition" regimes, linked by rapid transition regions.

3.2. Higher Spin Yrast States

The above results can be extended[9,10] to yrast states of much higher spins by using a 3-parameter generalization of eq. 2, namely

$$E(I) = nE(2_1^+) + \frac{n(n-1)}{2}\epsilon_4 + \frac{n(n-1)(n-2)}{6}\epsilon_6 \tag{3}$$

where ϵ_6 is a higher order parameter and $n = I/2$. This is equivalent to the general polynomial $E(I) = \alpha I + \beta^2 + \gamma I^3$ where α, β, and γ are free parameters. We fit the data for *all* even-even nuclei *including good rotors*, with $Z > 50$ and more than two nucleons of each type beyond closed shells up to the backbend or to the spin where the derivative of $\hbar\omega$ reverses direction (s-shaped behavior of I vs. $\hbar\omega$). $E(2_1^+)$ in eq. 3 is taken as a fitting parameter. Figure 5 shows a number of completely typical examples of the fits (not only the best cases) chosen to span as wide a range as possible of structures, mass ranges, and fit qualities. It is clear that in virtually every nucleus, regardless of structure, the AHV works at least as well as the best alternative approaches. Even in the actinides, where the data extend to $I \sim 28$, and $E = 5$ MeV, the discrepancies for the AHV are nearly always < 20 keV and, percentagewise, well below 1%. These results are particularly significant in rotational nuclei where the AHV is far superior to an expansion in powers of $I(I+1)$ (not shown because it is not even remotely competitive). The AHV is also at least as good as the Generalized VMI approach.

Were these results the full story, they might be dismissed as an interesting curiosity. However, yrast $B(E2)$ values also support the AHV approach. Generalizing ref. 11, we can write

$$B(E2; I \rightarrow I - 2) = \frac{1}{n}[nt_2 + \frac{n(n-1)}{2}t_4 + \frac{n(n-1)(n-2)}{6}t_6]^2 \tag{4}$$

where t_2, t_4 and t_6 are parameters. Several fits are shown in Fig. 5 for nuclei with a variety of $R_{4/2}$ values and behavior from linearly increasing, to parabolic, to s-shaped patterns. Nevertheless, the AHV expression gives excellent fits in all cases. No other geometric model we know has a single analytic expression for such a wide range of structures to show even for comparison. (The rotor expression is asymptotically flat at high spins and can account neither for a linear or parabolic shape, nor a trend reversal.) Of course, the upturn at high spin in the actinide $B(E2)$ values could, in principle, reflect a change of intrinsic structure, making the excellence of the AHV fit accidental. This may be the case, though we doubt it, and feel that the present results cannot be easily dismissed.
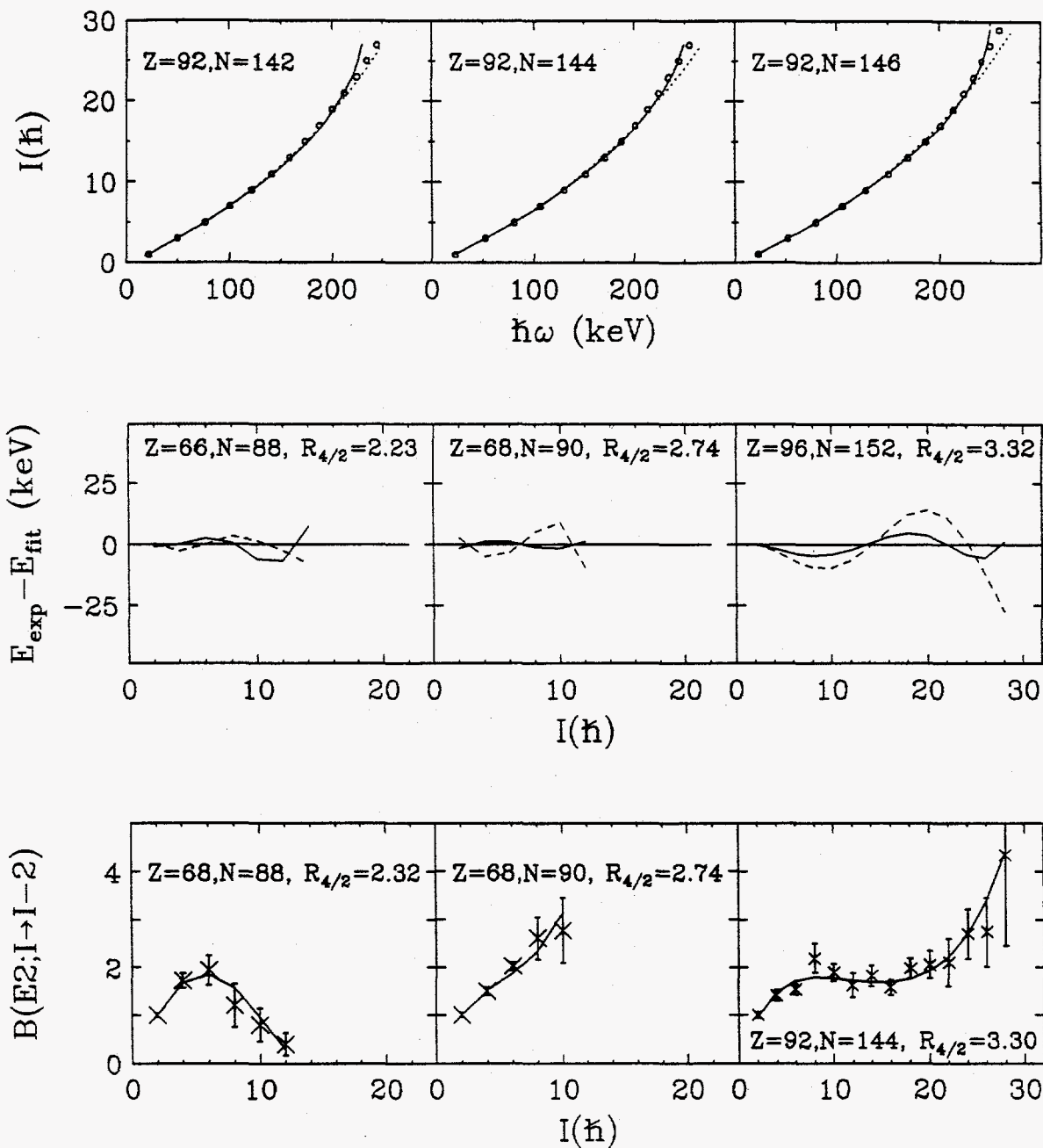
Fig. 5. Upper panels: Typical AHV (solid curves) and Generalized VMI (dahsed curves) fits to nuclei with structures from near harmonic vibrator to good rotor. Results are shown in two forms, I $vs.$ $\hbar\omega$ and $E_{exp} - E_{fit}$ $vs.$ I. The lowest panel shows AHV fits to yrast $B(E2)$ values. Based on ref. 10.

4. Exotic Nuclei

In exotic, near drip line nuclei, nuclear structure, as we know it, may be radically changed. Correlations such as we have been considering may or may not apply in such regions. If they do, they provide an evolutionary paradigm that will be invaluable. If they do not, the breakdown of these correlations will itself signal the radical structural changes anticipated.

The neutron rich side of stability is especially interesting due to the longer "lever arm" from the valley of stability and to the exotic phenomena expected. Near the neutron drip line, the outer realms of nuclei comprise an extended, diffuse, low-density region of nearly-pure neutron matter. As suggested recently[12,13], such a diffuse density distribution is unlikely to support a shell model potential with sharp contours. Hence, even the traditional form of the Shell Model Hamiltonian itself may be radically altered. Its Woods-Saxon form may go over into a more rounded harmonic oscillator shape. In the language of the Nilsson model, this corresponds to the vanishing of the "l^2" term.

The consequences of this are hard to overestimate. Consider the single particle levels in such a scenario (Fig. 6, right). The energy of the unique parity orbit increases to return to its parent shell. Hence, magic numbers change and high spin phenomena and octupole correlations will be dramatically altered since they depend in essential ways on the location of these special orbits. But, more profound changes occur. The traditional order of the normal parity orbits (see Fig. 6, center), namely a monotonical decrease in j with $\Delta j = -1$ is completely upset. Instead, one encounters a "nested" pattern of j orbits with the highest j orbits surrounding the middle j, which in turn enclose still lower j orbits. Moreover, the j spin sequence is now $\Delta l = \Delta j = -2$ throughout. Manifestations of collectivity, and especially its evolution with N and Z, could be significantly different than near stability since the quadrupole interaction has particularly large matrix elements that couple orbits with $\Delta l = \Delta j = 2$.

In addition, the weak binding of the outermost neutrons and the proximity of quasi-bound continuum levels means that coupling to continuum states must be considered. Moreover, as the uppermost orbits in a shell merge into the continuum (perhaps as quasi-bound levels) the remaining bound levels no longer constitute a complete sequence of j values from some j_{max} down to $j = 1/2$. The distorted single j-shell sequences, and the merging into and coupling with the continuum, could easily change symmetries [such as $SU(3)$ or pseudo- $SU(3)$] associated with the fermionic states. Residual interactions will also be different. The pairing interaction connecting weakly bound or continuum states that are greatly extended in space, could become significantly stronger[12,13]. At the same time, the vast neutron excess and the difference in proton and neutron orbits will alter the $p - n$ interaction.

Figure 6 also illustrates an alternate scenario of possible changes in the Shell Model in nuclei far from stability, namely the absence of the spin orbit interaction. This scenario could characterize some neutron rich nuclei or perhaps only the proton orbits inside the diffuse neutron skin.

We will discuss three applications of horizontal correlations to the structure of exotic nuclei: the use of $B(E2 : 2_1^+ \rightarrow 0_1^+)$ values (hereafter, "$B(E2)$" values) to identify magic numbers in new regions and to disclose subtle aspects of nuclear shapes, and the use of the energy ratio $E(4_1^+)/E(2_1^+)$ to give clues to Shell Model single-particle level sequences.
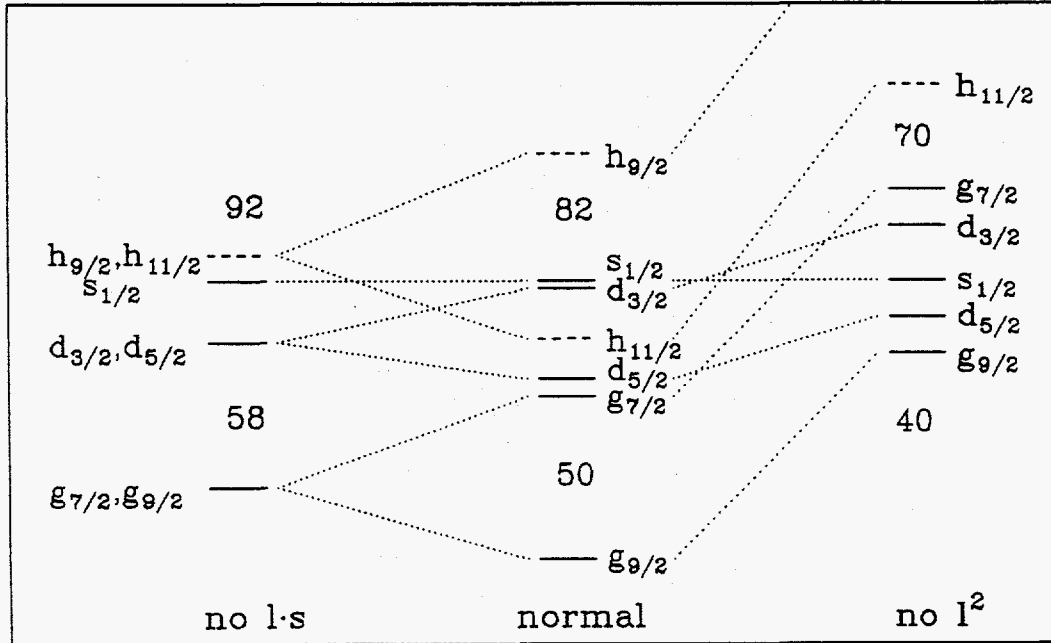

Fig. 6. Normal (middle) and exotic scenarios for single particle energies (see text).

4.1. B(E2) values and magic numbers

The basic idea is that $B(E2)$ values behave simply in $N_p N_n$ plots. Of course, a previso for this is an accurate counting of $N_p N_n$. If shell structure is altered from that defined by the traditional magic numbers, or is unknown, the use of incorrect N_p and N_n values can generate large deviations from simple patterns. Figure 7 illustrates this for the $A \sim 100$ region.[14] On the left, the standard magic numbers are used, namely $Z = 40, 50$ for $50 < N < 60, Z = 28, 50$ for $N \geq 60$. A compact, indeed linear, correlation is achieved. If the well known subshell at $Z = 40$ for $N < 60$ were *not* assumed, however, the correlation becomes messy (Fig. 7, middle). Suppose further that $Z = 50$ is not taken as a magic number. Then the plot on the right of Fig. 7 is obtained. Clearly, the compact correlation for $B(E2)$ values against $N_p N_n$ is destroyed. Even in advance of specific level scheme data on ^{100}Sn, this certainly suggests that the $Z = 50$ proton shell closure is intact, at least for nuclei within a few proton or neutron numbers of 50.
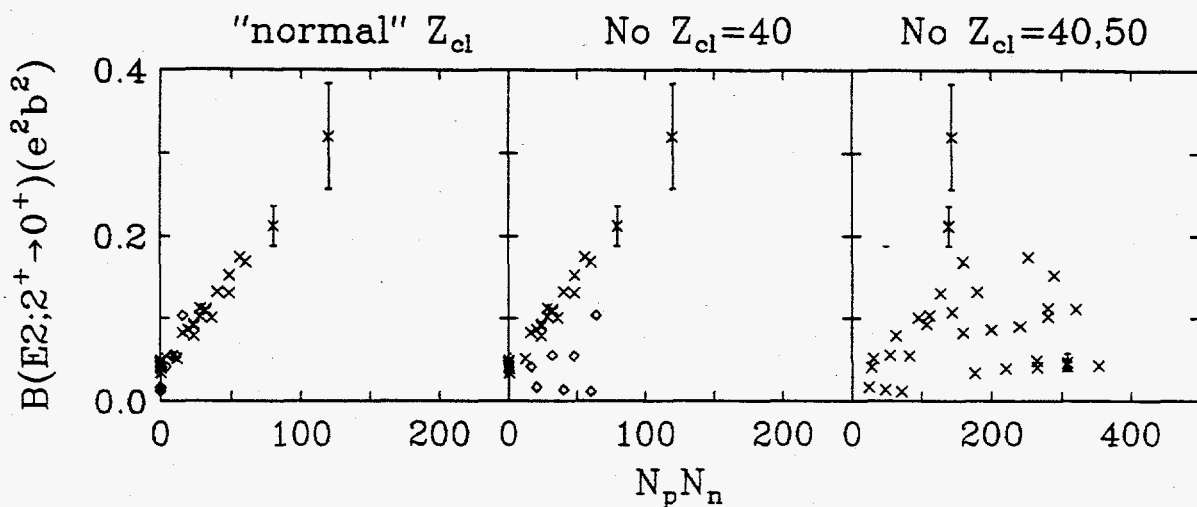
Fig. 7. Use of $B(E2)$ values to test the validity of magic numbers[14]. See text.

4.2. Hexadecapole deformations and B(E2) values

Figure 8a shows $B(E2)$ values against $N_p N_n$ for all even nuclei with $Z > 28$. Although the correlation is simpler than one against N or Z, it is not as simple as others we have considered. This is a manifestation of hexadecapole deformations (β_4). To see this, note the relation for the quadrupole moment

$$Q(2^+) \sim \beta_2(1 + 0.3604\beta_2 + 0.9672\beta_4 + 0.3277\frac{\beta_4^2}{\beta_2} + ...). \qquad (5)$$

Q depends on β_4 and on its sign. Since $\sqrt{B(E2)} \propto Q$, the $B(E2)$ values do also. In any major shell β_4 deformations have a characteristic systematics. They are large and positive early in a shell, cross zero near mid-shell and then turn large and negative. Thus, from eq. 5, we see that $B(E2)$ values are increased by the effects of hexadecapole deformations early in a shell and decreased later on. This leads to the curvatures evident in Fig. 8a. If, however, the effects of β_4 deformations are *removed* from the $B(E2)$ values (by moving the β_4 terms to the left hand side of eq. 5), giving the values that *would* arise if β_4 were zero, the resulting $B(E2)$ values are nearly straight against $N_p N_n$ shown in Fig. 8b.
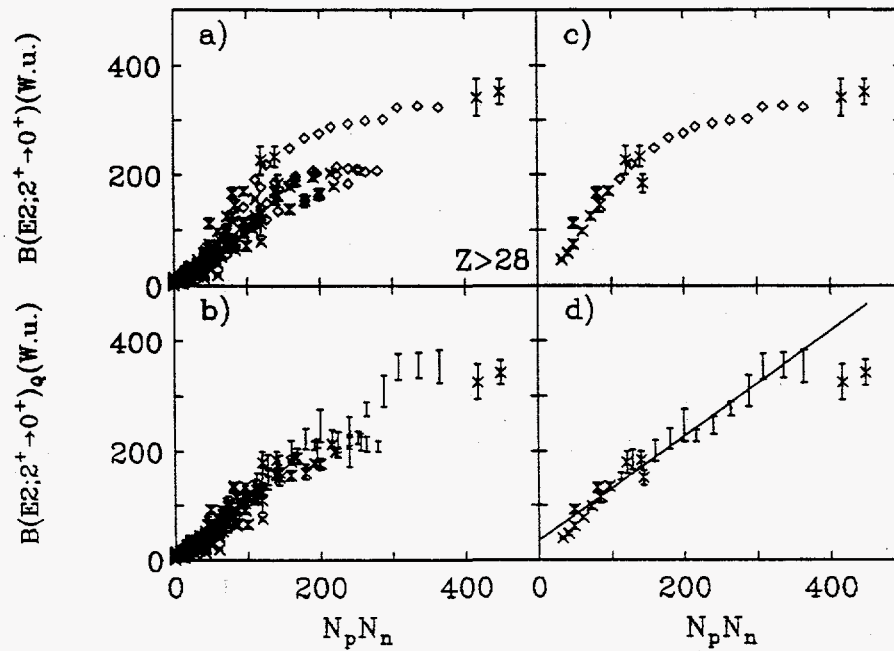
Fig. 8. (Top) $B(E2)$ values against $N_p N_n$. (Bottom) $B(E2)_Q$ values [i.e., $B(E2)$ values corrected for β_4—see text] against $N_p N_n$. Based on ref. 15. Crosses denote nuclei where β_2, β_4 values from ref. 16 were used to correct $B(E2)$ values: in all these cases, empirical β_2, β_4 values were used.

The linear trajectory means that if $B(E2)$ values are measured in new nuclei, deviations from such trajectories can be used to estimate unknown β_4 values[15]. Figures 8c,d illustrates this by showing $B(E2)$ and $B(E2)_Q$ values for actinide nuclei. Clearly the $B(E2)_Q$ values lie on a nearly straight line trajectory. We note that, at the far right of Fig. 8d, the $B(E2)$ values for ^{250,252}Cf fall well below the trendline. One can estimate the required β_4 to move these two points to the line. We obtain $\beta_4 \sim -0.07$. Interestingly, theoretical calculations do not give a negative value. Thus, not only do we extract a semi-quantitative estimate of β_4, but we can address possible improvements to calculations of the heaviest elements.

4.3. Shell structure and $E(4_1^+)/E(2_1^+)$ ratios in magic nuclei

Finally, we consider a simple approach to gleaning clues to underlying j-shell structure. Consider a shell model configuration $| j^2 J >$. The energies of the levels $J = 0, 2, 4 \ldots (2j - 1)$ under a short range residual interaction have a characteristic pattern. The 0^+ level is greatly lowered, and the higher spin states cluster not far below their unperturbed positions. $R_{4/2} \sim 1.2$ and is nearly independent of j. (The same result applies to multi-j configurations of the type $| j_1^{n_1} J_1, j_2^{n_2} J_2, \ldots > (n_i$

even).) The reason is that only in the 0^+ state are the angular momenta of the two nucleons co-planar and the spatial wave functions symmetric. Hence the particles are in close enough contact to be affected by a short range interaction. From this, one would expect such $R_{4/2}$ values to be characteristic of nuclei with 2 nucleons of the same type outside closed shells. However, it is only in heavy nuclei (e.g., ^{210}Pb, ^{210}Po) that this is approximately realized. In lighter nuclei (e.g., ^{18}O), $R_{4/2}$ can be as large as 1.7. In fact, the data on $R_{4/2}$ in singly magic nuclei are quite regular, as shown in Fig. 9a.
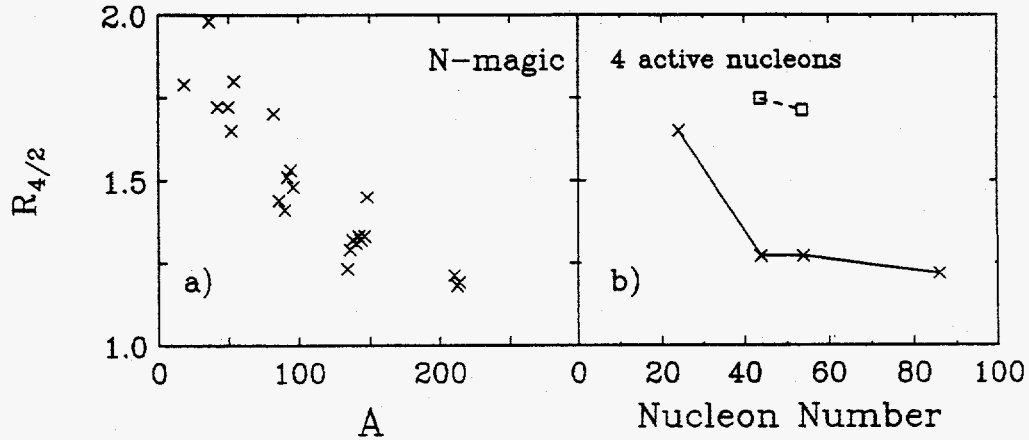

Fig. 9. a) Empirical $R_{4/2}$ values for neutron magic nuclei. b) SDI calculations [17] of $R_{4/2}$ for normal shell model sequences (solid line) and for the "no-l^2" scenario (squares).

A simple model[17] helps us understand both the high $R_{4/2}$ values in light magic nuclei and the use of $R_{4/2}$ to study the underlying j-shell structure in new mass regions. Consider, instead of configurations involving pairs of particles, a situation with two nucleons, one in each of two orbits, that is, $\mid j_1, j_2 J >$. If $\mid j_1 - j_2 \mid \neq 2$, the pattern of even spin levels that results is similar to the $\mid j^n J >$ case, with $R_{4/2} \sim 1.2$. Now, however, consider the unique case of $\mid j_1 - j_2 \mid = 2$. Here, the 2^+ state is formed (semi- classically) by co-planar orbits. Hence the attractive residual interaction has large effect, and the 2_1^+ level is strongly lowered, raising $R_{4/2}$. Such wave function components, with *odd* numbers of nucleons in each of two orbits with $\mid j_1 - j_2 \mid = 2$, help explain the large $R_{4/2}$ values in light singly magic nuclei since in these nuclei the typical j-shell is in fact $\Delta j = 2$ [e.g., the $s - d$ shell with $d_{5/2} - s_{1/2} - d_{3/2}$]. In new neutron-rich mass regions accessible with RNBs, where $\Delta j = 2$ shell patterns such as in Fig. 6 (right) may appear, the easiest signature of such sequences may therefore lie simply in measuring $R_{4/2}$ values in singly magic nuclei. Anomalously large values would signal $\Delta j = 2$ sequences. Figure 9b shows surface δ function calculations that illustrate this. The solid line is obtained with normal shell structure. Note the larger $R_{4/2}$ values for lighter nuclei and the falloff as $\Delta j = 1$ sequences appear in heavier nuclei. Clearly, these shell model calculations, though schematic and highly simplified, do mimic the data in Fig. 9a. If we now

assume the scenario on the right in Fig. 6 for mid-mass nuclei, $\Delta j = 2$ amplitudes will be larger and anomalously high $R_{4/2}$ values will result. Re-calculating $R_{4/2}$ for this case gives the two higher lying points in Fig. 9b.

5. Summary

Despite the apparent complexity of nuclear phenomenology, extraordinarily simple, "horizontal", correlations of data reveal regular evolutionary behavior. Correlations with secular variables such as $N_p N_n$ or P, or between collective observables themselves, are useful. The correlations provide powerful new signatures of structure that will be particularly useful in new nuclear regions that will become accessible with radioactive nuclear beams.

6. Acknowledgments

7. References

1. P. Federman and S. Pittel, Phys. Lett. **69B** (1977) 385, **77B** (1978) 29. A. de Shalit and M. Goldhaber, Phys. Rev. **92** (1953) 1211; I. Talmi, Rev. Mod. Phys. **34** (1962) 704.
2. R.F. Casten, Nucl. Phys. **A443** (1985) 1.
3. R.F. Casten, D.S. Brenner, P. Haustein, Phys. Rev. Lett. **58** (1987) 658.
4. B. Foy et al., Phys. Rev. **C49** (1994) 1224.
5. R.F. Casten, N.V. Zamfir, D.S. Brenner, Phys. Rev. Lett. **71** (1993) 227.
6. N.V. Zamfir and R.F. Casten, Phys. Lett. **B341** (1994) 1.
7. N. Pietralla et al., Phys. Rev. Lett. **72** (1994) 2962.
8. N.V. Zamfir, R.F. Casten, D.S. Brenner, Phys. Rev. Let. **72** (1994) 3480.
9. T.K. Das, R.M. Dreizler and A. Klein, Phys. Rev. **C2** (1970) 632.
10. N.V. Zamfir and R.F. Casten, Phys. Rev. Lett. **75** (1995) 1280.
11. D.M. Brink, A. de Toledo Piza, A.K. Kerman, Phys. Lett. **19** (1965) 413.
12. J. Dobaczewski et al., Phys. Rev. Lett. **72** (1994) 981.
13. W. Nazarewicz et al., Phys. Rev. **C50** (1994) 2860.
14. R.F. Casten and N.V. Zamfir, Physica Scripta **T56** (1995) 47.
15. N.V. Zamfir et al., Phys. Lett. B (in press).
16. P. Möller et al., At. Data Nucl. Data Tables **A59** (1995) 185.
17. R.F. Casten, N.V. Zamfir, D.S. Brenner, Phys. Lett. **B324** (1994) 267; **B342** (1995) 451; W.-T. Chou, R.F. Casten, N.V. Zamfir, Phys. Rev. **C51** (1995) 2444.